

Journal of Hydraulic and Water Engineering (JHWE)



Journal homepage: https://jhwe.shahroodut.ac.ir

Stability Analysis and Sensor-Based Monitoring of Earthen Dams in Semi-Arid Regions: A Case Study of Daroongar Dam, Iran

Farzin Salari ¹, Mobin Eftekhari ^{2*}, Abbas Ali Ghezelsofloo ³

- ¹ Civil Engineering, Water and Hydraulic Structures, Young Researchers and Elite Club, Mashhad Branch, Islamic Azad University, Mashhad, Iran.
- ^{2*} Department of Water Engineering, University of Birjand, Birjand, Iran.
- ³ Civil Engineering Department, Mashhad Branch, Islamic Azad University, Mashhad, Iran.

Article Info

Article history: Received 16 April 2025 Received in revised form 25 May 2025 Accepted 01 August 2025 Published online 07 August 2025

DOI: 10.22044/JHWE.2025.16080.1061

Keywords

Monitoring of Earth Dams Stability Instrumentation Total stress Arching

Abstract

This study presents a comprehensive stability assessment of the Daroongar earth dam in Iran's semi-arid region through a 3-year monitoring program (2019-2022) that combines precision instrumentation and finite-element modeling (Plaxis 8.6). Field data from 19 embankment piezometers, 10 electric piezometers, 28 standpipe piezometers, and 13 total pressure cells installed in critical sections were systematically analyzed. Comparative analysis of key parameters revealed significant discrepancies between field measurements and numerical simulations: total stress showed 22% average deviation, pore pressure in the dam body exhibited 37.9% mismatch, while foundation pore pressure demonstrated a 35% discrepancy ($\Delta = 304.3 \text{ kN/m}^2$, p<0.05), primarily attributed to instrument blockages. Arching effects analysis indicated minor 0.032 unit variations (95% CI: -0.3-0.37), within acceptable safety limits. The research highlights the importance of shorter monitoring intervals and the use of thermometric methods to enhance seepage detection. Statistical validation via SPSS emphasized the need for constitutive model recalibration, particularly for soil-specific gravity and shear strength parameters, to reduce simulation-field measurement gaps. Practical recommendations include proactive maintenance protocols addressing instrument blockages and optimized drainage system designs. These findings provide actionable insights for improving the safety and longevity of earth dams in semiarid climates, demonstrating the critical synergy between advanced numerical modeling and robust field instrumentation systems. The study contributes to a better understanding of earth dam behavior under operational conditions while proposing concrete measures to enhance monitoring accuracy.

1. Introduction

Structural behavior monitoring involves evaluating a structure's performance during both construction and operational phases, while comparing actual measurements with design specifications. Among engineering civil structures, earthen dams require particularly rigorous behavior analysis due to their critical performance importance and complex monitor characteristics. Engineers these structures using precision instrumentation systems, in which specialized sensors record structural responses, which are then converted into quantitative data by transducers. Historically, before the early 20th century, major infrastructure consisted primarily of bridges, tunnels, aqueducts, and canals, constructed mainly of wood and metal. Maintenance of these structures followed a compartmentalized approach, with dedicated agencies overseeing specific sectors in a highly segmented manner. Maintenance personnel

typically focus on discrete structural components, developing specialized knowledge about their assigned elements. This localized maintenance paradigm contemporary understanding of risk assessment and damage prevention, as structural integrity management remained intrinsically tied to the construction context (Salin original al.,2018). The Daroongar Dam, a 40-meterhigh clay-core earth dam in Northeast Iran, is critical for flood control and irrigation in a semi-arid region. Semi-arid challenges include rapid desiccation cracks (e.g., seasonal width variation of 2-5 cm) and flash-flood-induced hydraulic shocks, as observed in Iranian embankments (Al-Ansari et al., 2021), complicating the dam's seepage and stress behavior and necessitating robust monitoring and modeling to ensure stability. This study employs field instrumentation and Plaxis 2D finite element modeling to assess total stress, pore pressure, and arching effects, addressing discrepancies and informing long-term safety. The emergence of mega-structures in the early necessitated 20th century standardized technical frameworks. In 1928, this led industry establish International leaders the Commission on Large Dams (ICOLD), which systematically developed unified protocols for construction, monitoring, and operational procedures (Salin et al., 2018). Through these collaborative efforts, monitoring practices became increasingly rationalized, particularly through the refinement of non-destructive testing (NDT) techniques. While accumulated structural knowledge has informed numerous regulations and standards, these guidelines primarily support design and construction phases rather than operational monitoring. Historically, effective monitoring relied on specialized professionals providing continuous structural assessments to decision-makers. This practice fostered networks of experts that ultimately led to the establishment of dedicated structural monitoring institutions (Riveiro & geotechnical Solla, 2016). As critical infrastructure, dams primarily serve water storage functions. However, some facilitate tailings management in mining operations.

ICOLD data indicates embankment dams represent approximately 78% of all dam structures worldwide (Rana et al., 2022). These embankments further classify into: Earth/soil dams (83%) and Rockfill dams (17%). Both types employ various waterproofing systems, including concrete facings or clay cores (Rana et al., 2022). Effective dam design must account for diverse environmental and operational conditions to ensure long-term structural stability and safety (Bashar et al., 2023). The evaluation of dam safety parameters necessitates rigorous computational analysis accounts various site-specific for uncertainties during the design phase (Deneale et al., 2019). Proper protection, maintenance, and operation of dams are crucial not only for ensuring structural longevity but also for safeguarding public health, safety, and the environment (Adamo et al., 2021). However, one of the most significant challenges in major infrastructure projects stems from inadequate maintenance procedures (Mazele & Amoah, 2022). Given the substantial costs and extended timelines associated with dam construction, implementing comprehensive a monitoring and maintenance program becomes essential. Such systems enable early detection operational defects structural and abnormalities, which are vital for integrity assessment, continuous health monitoring, and management. Accurate effective risk simulation of dam behavior during construction precise measurement requires of parameters, including displacement, pore water pressure, and leakage rates, which can be achieved through specialized monitoring instrumentation (Hui et al., 2018). Health monitoring procedures are particularly valuable when integrated with risk analysis frameworks to identify Potential Failure Modes (PFMs) (Liu et al., 2020). By combining these identified failure modes with continuous monitoring data, engineers gain critical insights structural performance, hydraulic into behavior, and geotechnical conditions. Advanced post-processing of this data further enhances the reliable determination of PFMs, supporting proactive maintenance and risk

mitigation strategies (Cong & Inazumi, 2024). research Extensive has established comprehensive recommendations for monitoring and analyzing earth dams and levees (Ceika et al., 2018). instrumentation systems enable measurement of diverse physical and mechanical parameters critical to geotechnical engineering and construction projects (Jastrzębska, 2021), with particular focus on quantifying variations in displacement and water pressure through instrumented data collection (Van Stan et al., 2013). Strategic placement of these monitoring devices at sensitive dam locations, coupled with advanced measuring equipment and online data acquisition systems, forms the foundation for rigorous dam safety assessments (Adamo et al., 2021). Given that structural failures in earth and rockfill dams can cause catastrophic downstream consequences, performance must be continuously evaluated using multiple behavioral indicators, including pore-water pressures, stress distributions, displacement patterns, and other critical parameters, during health-monitoring programs. These require assessments systematic interpretation and reporting, with special protocols for emergency scenarios such as floods or earthquakes (Wu et al., 2023). Dam stability evaluation fundamentally relies on a comparative analysis of current performance against historical behavior patterns (Salazar et al., 2017), while risk assessment methodologies may be applied at various scales—from regional dam portfolio analyses advanced numerical simulations and experimental investigations (Wang et al., 2023). Behavior monitoring encompasses a comprehensive evaluation of structural performance throughout the construction and operational phases, verifying the actual response against design predictions. For earthen structures, this monitoring particularly crucial due to potential failure mechanisms including slope instability, seepage-induced erosion, hydraulic fracturing, and particle migration (Soltaninejad et al., 2025). Effective monitoring requires deployment of multiple instrumentation

systems to detect environmental and structural with analysis parameters changes, key encompassing water stability-runoff relationships, implementation design verification, geometric characteristics (shape, height), foundation and abutment performance, drainage efficiency, thermal effects, and seismic response (Xiong & Huang. 2019). The practical implementation of these principles is demonstrated through core instrumentation systems that monitor dam behavior during both construction and operational phases, including during reservoir filling and drawdown (Adamo et al., 2021). The collected data enables continuous evaluation of structural response, forming the basis for informed safety management decisions. The analytical results have been systematically validated against data from precision instrumentation systems, with continuous monitoring of the dam's body and foundation providing a comprehensive operational performance assessment (Márquez López, 2023). Current challenges in dam safety management underscore the critical role of behavior mapping in earthen dams, where complex mechanical responses necessitate integration into holistic stability-control programs. As established by the ASCE Committee (2000), proper instrumentation deployment during both construction and initial operation phases enables effective evaluation of key performance variables, while predictive behavior modeling can significantly mitigate risks by identifying potential failure modes before occurrence (Chen & Chen.2015) These capabilities are particularly crucial given that approximately 80% of operational dams in the country utilize gravel-type construction - a design representing over 75% of historical dam worldwide. socioeconomic The imperative for rigorous safety monitoring becomes evident when considering catastrophic consequences of dam failures, including devastating flash floods that lead to irreplaceable water resource losses, substantial reconstruction costs, environmental destruction, population and downstream displacement. Periodic performance evaluation operational dams using advanced instrumentation systems is, therefore, essential to enhance monitoring protocols and safety standards. Earthen and gravel dams are particularly vulnerable to multiple failure mechanisms, including changes in total stress, arching effects, fluctuations in pore-water pressure, seepage forces, and differential settlements. Accurate investigation of these fundamentally requires: phenomena properly calibrated instrumentation systems, (2) rigorous data analysis protocols, and (3) expert interpretation of results. This tripartite requirement underscores that neither construction quality assurance nor operational safety monitoring can be effectively conducted without sophisticated monitoring tools and skilled technical personnel. The findings collectively highlight the necessity continued advancements in dam monitoring technologies and analytical methodologies to address the complex behavior of earthen structures throughout their lifecycle. Recent have witnessed significant decades advancements in dam monitoring technologies. Salin et al. (2018) demonstrated the efficacy of non-destructive testing (NDT) methods for detecting stress variations in infrastructure. Building on this, Bartholomew established Murray comprehensive guidelines for instrumentation placement, emphasizing the importance of sensor networks in high-risk zones. Lindsey et al. further validated the role of automated systems in enhancing measurement accuracy for such as pore pressure parameters displacement. At the same time, Dunnicliff's seminal work laid the foundation for modern geotechnical instrumentation protocols. These

2. Materials and Methods

The research methodology integrated numerical modeling with field monitoring to assess the performance of the Daroongar Dam. The computational analysis commenced with geometric modeling of the dam foundation in Plaxis 8.6, incorporating critical boundary conditions, including full fixity constraints at the base and roller supports along vertical boundaries to simulate realistic deformation

studies collectively underscore the need for robust monitoring systems to enable early anomaly detection. Finite element modeling has become a cornerstone in dam stability assessment. Athani et al. 2015 pioneered the application of this method to evaluate seepage effects on slope stability, revealing critical relationships between hydraulic forces and structural integrity. Mouyeaux et al. (2018) expanded on these efforts by integrating probabilistic approaches to account geotechnical uncertainties, thereby significantly improving failure-prediction accuracy. Advanced numerical simulations by Farias and Cordão Neto 2010 further demonstrated the ability to predict dam behavior under diverse loading conditions, highlighting the importance of constitutive model calibration. These methodologies form the basis for contemporary risk assessment frameworks. Despite progress, critical gaps persist in understanding gravel-type dam behavior in semi-arid regions. While Wang et al. (2020) investigated sedimentation dynamics in tailings dams, the hydraulic responses of water-retaining gravel dams under arid conditions remain underexplored. Similarly, Huang et al. 2018 focused on concrete dam displacements but overlooked the unique challenges of earthen structures. This study addresses these gaps by combining Plaxisbased finite element analysis with continuous instrumentation data from the Daroongar Dam case study. By synthesizing methodologies from Guo et al. (2019) and Hariri-Ardebili's (2018) risk assessment frameworks, advance predictive capabilities for gravel-type dams in water-scarce environments.

patterns. Soil behavior was simulated by assigning material-specific strength parameters (elastic modulus, Poisson's ratio, cohesion, and friction angle) to each geometric zone, followed by the generation of a finite element mesh using 6-node triangular elements with refined discretization in critical zones to ensure solution accuracy. The model domain was extended laterally by three times the dam height in all directions to minimize boundary

effects, following established geotechnical modeling practices. This study compares three years (2019-2022) of instrumentation data with numerical simulation results through comprehensive monitoring system comprising 19 embankment piezometers foundation piezometers (RP), 13 total pressure cells (TPC), and 28 standpipe piezometers (SP) installed in critical sections. Electronic instruments recorded automated measurements twice monthly (5th and 14th), while manual instruments were read monthly, with additional dewatering observations during and operational events. The instrumentation system served to validate design assumptions, assess structural performance during construction, initial reservoir filling, and the operational phases, and identify potential failure modes through displacement analysis, pore pressure monitoring, stress redistribution and Statistical evaluation. validation was performed using SPSS (v26) with paired t-tests quantify differences between and numerical predictions. measurements thereby ensuring a robust comparison of observed and simulated behavior across various loading conditions.

2.1. Case Study

The Daroongar storage dam, located in the Ooch-Meydan valley, 35 km northwest of Dargaz in Iran's Khorasan Razavi province, is a critical piece of water management infrastructure in this semi-arid region. This engineered structure features a vertical clay core supported by an alluvial foundation, reaching a maximum thickness approximately 40 meters at key sections. During construction, significant dewatering efforts lowered the natural groundwater table beneath the core zone to depths exceeding 15 meters to ensure proper compaction and stability. Designed primarily for flood control in the watershed, the dam serves dual purposes: regulating seasonal river flows and providing essential water storage for agricultural irrigation in downstream areas. The selected site conditions and structural configuration reflect careful consideration of the region's hydrologic characteristics and geotechnical constraints, with the clay core design optimizing both seepage control and structural integrity under variable loading conditions. The 2D model was selected for its crosscomputational sectional symmetry and efficiency, as 3D effects (e.g., transverse stress) were deemed negligible for the global behavior analysis. This case study examines both operational performance and monitoring data from a representative example of earth-dam engineering in arid environments.

Table 1. Specifications of the body and foundation materials of Daronagar dam based on the design data (Ministry of Energy - Khorasan Regional Water Joint Stock Company)

	Specif	ic gravity	shear strength parameters		
aggregate	Humid (t/ m3)	Saturation (t/ m ³)	Stickiness (kg/ cm ²)	The angle of internal friction (degrees)	
Shell	2.1	2.17	0.0	40	
Core:					
UU	2.05	2.12	0.35	5	
CU	2.03	2.12	0.35	17	
CD			0.14	26	
Foundation: Fine-grain unit: Saturation CU CD	1.9	2.01	0.34 0.1	0.17 26	
Coarse-grain unit:	1.9	2.01	0.1	26	

Table 1 presents the geotechnical specifications for the materials used in the construction of the Daroongar Dam, as documented in the original design reports of the Khorasan Regional Water Company [31]. The data systematically organize key parameters for each structural component — shell, clay core, and foundation materials — with particular attention to their shear strength characteristics. For the clay core, the table differentiates between three testing conditions (UU, CU, and CD), showing how shear strength parameters vary significantly with drainage conditions - from a cohesion of 0.35 kg/cm² in UU/CU tests to 0.14 kg/cm² in CD tests, while the friction angle increases

from 5° to 26°, respectively. The foundation materials exhibit similar trends, with finegrained units showing higher cohesion (0.34 kg/cm²) compared to coarse-grained units (0.1 kg/cm²) under consolidated undrained conditions. Notably, the shell material demonstrates typical granular behavior with zero cohesion and a high friction angle of 40°, reflecting its free-draining nature. These carefully measured parameters formed the basis for the dam's stability analysis and were subsequently validated through instrumentation during construction and operation.

Table 2. Material characteristics of the body and foundation of the dam in stress-strain analysis using the finite element method (Toossab Consulting Engineering Company)

aggregate	Specific gravity (KN/ m³)	E(Kpa)	v	C (Kpa)	ø (degree)	Ko			
	(IXI Vi III)	, , , , , , , , , , , , , , , , , , ,	Zone 1- core	 e					
In mode U.U.		26800	0.48	35	5				
In mode C.U.	20.0	26800	0.48	35	17				
In mode C.D.		22300	0.25	14	26				
		Z	one 2 - shel	ls					
	21.0	40000	0.2	-	40				
Zone 3 - alluvial base									
In mode C.U.	10.0	204000	0.48	34	17	0.5			
In mode C.D.	19.0	17000	0.3	(40-10)40	26	0.5			

Table 2 details the material characteristics used for finite element analysis of the Daroongar Dam, as provided by Toossab Consulting Engineering Company [32]. The

table systematically presents stress-strain parameters for the dam's core, shells, and alluvial foundation under various testing conditions (UU, CU, and CD). Key parameters include elastic modulus (E) ranging from 17,000 kPa for the foundation in CD condition to 40,000 kPa for the shells, Poisson's ratio (v) varying between 0.2 for shells and 0.48 for the core in UU/CU conditions, cohesion (c) values from 14 kPa for the core in CD to 40 kPa for the foundation, and friction angles (φ) spanning 5° to 40°. The table also includes the coefficient of earth pressure at rest (K_0) for foundation materials. These carefully

calibrated parameters, particularly the differentiation between undrained and drained conditions for the clay core (which showed significant variations in stiffness strength), were essential for accurately predicting the behavior during dam's construction and operation. The data reflect the comprehensive laboratory and field investigations conducted to characterize the nonlinear, stress-dependent behavior of earth materials in this critical infrastructure project.

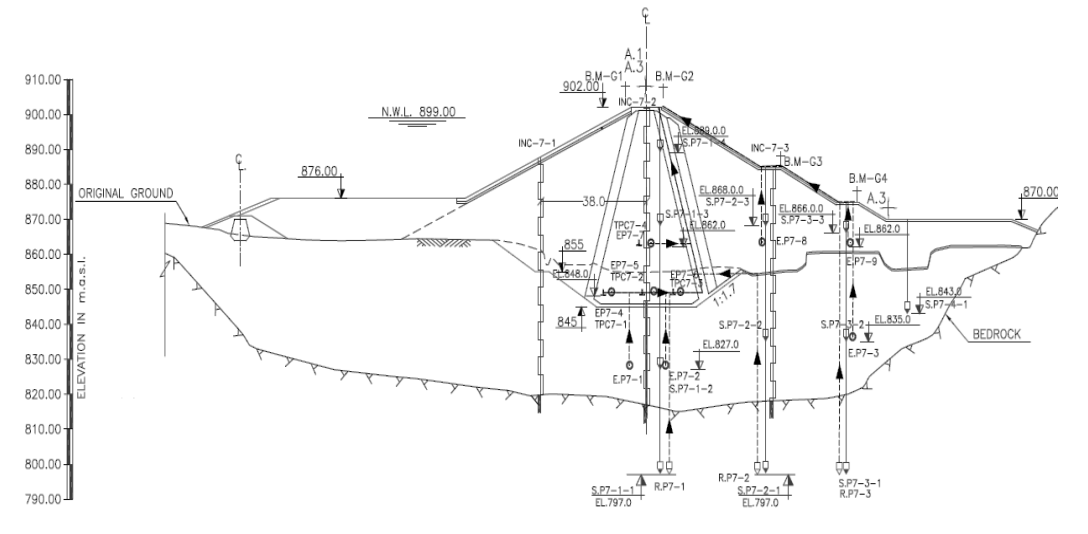


Figure 1. Section 7a with the available precision tools

Figure 1 presents a cross-sectional view (Section 7a) of the Daroongar Dam showing strategic placement of the precision instrumentation within both the embankment foundation layers. The schematic and illustration highlights the configuration of key monitoring devices, including: (1) electrical piezometers (EP) embedded within the clay core, (2) total pressure cells (TPC) distributed across critical zones of the dam body, and (3) standpipe piezometers (SP) installed in the alluvial foundation. The instrumentation network specifically targets sensitive locations, such as beneath the clay core, adjacent to drainage systems, and at the interface between the granular shell and foundation, enabling simultaneous monitoring of critical parameters, including pore water

pressure, total stress, and potential seepage paths. This optimized sensor arrangement was determined through preliminary behavioral analysis of the dam structure, focusing on identifying potential deformation zones and stress-concentration areas. The systematic instrumentation layout serves as fundamental basis for correlating field measurements with finite element modeling thereby validating predictions, assumptions and operational performance criteria. The figure particularly emphasizes the vertical alignment of instruments along potential seepage paths and stress transfer reflecting comprehensive zones. the monitoring strategy adopted for this embankment dam.

Table 3. Instrumentation predicted for the Daroongar dam

Row	Instrumentation	Symbol	Total	Number in Section 7a	Description
1	Electric embankment piezometer	E.P.	19	9	-
2	Electric piezometer	R.P.	10	3	These tools are connected to the central reading system.
3	Standing pipe piezometer	S.P.	28	11	-
4	Total pressure gauge cell	T.P.C.	13	4	-

Table 3 provides a comprehensive overview of the instrumentation system implemented at Daroongar Dam, detailing the quantities, and distribution of monitoring devices across the structure. The table categorizes four primary instrument groups: 19 electric embankment piezometers (E.P.) with 9 units installed in Section 7a, 10 electric foundation piezometers (R.P.) including 3 in Section 7a, 28 standpipe piezometers (S.P.) with 11 in the study section, and 13 total pressure gauge cells (T.P.C.) featuring 4 units in Section 7a. A critical feature highlighted in the table is the centralized data-acquisition system that links all electronic instruments, enabling real-time monitoring of hydraulic and mechanical responses. The instrumentation plan demonstrates a particular concentration in Section 7a, selected as the representative cross-section due to its geological characteristics and structural importance, which contains approximately 40% of the total electronic monitoring devices. This strategic distribution reflects the design priorities for detecting potential core piezometers), cracking (via redistribution (through pressure cells), and foundation seepage (monitored standpipes). The table essentially serves as the blueprint for the dam's behavioral monitoring framework, correlating directly with the numerical modeling validation methodology presented in the study. The research methodology focused on a comprehensive analysis of the Daroongar Dam's behavior through detailed instrumentation numerical modeling. During preliminary investigations, four critical cross-sections (3a, 7a, 11a, and 14a) were evaluated based on

their structural characteristics, instrumentation coverage, and geotechnical significance. Section 7a emerged as the most representative and strategically important location due to several key factors: its typical cross-sectional geometry reflects the dam's overall design, it contains the full array of monitoring instruments (including piezometers, pressure cells, and standpipes), and it captures both the maximum embankment height and critical foundation conditions. This section's comprehensive instrumentation network and central location within the dam structure make it an ideal control section for evaluating the dam's response to various loading conditions. The selection of Section 7a allows for systematic comparison between field measurements and numerical predictions while ensuring the findings can be reasonably extrapolated to understand the global behavior of the entire dam structure. The methodology combines data from this representative section with advanced finite-element analysis to provide a comprehensive assessment of the dam's performance during both construction and operational phases. geotechnical The modeling process was conducted using Plaxis finite software. element incorporated the essential geotechnical and geometric parameters derived from Section 7a to establish a representative numerical model of the Daroongar Dam. The software's advanced constitutive models enabled accurate simulation of the dam's multilayered structure, including the clay core, granular shells, and alluvial foundation, by integrating key material properties—elastic moduli, Poisson's ratios, and shear strength parameters

—derived from laboratory and field tests. The model geometry precisely replicated the cross-sectional dimensions and boundary conditions of Section 7a, and the mesh generation used 6-node triangular elements with localized refinement in critical zones to ensure computational accuracy. This modeling framework, grounded in the characteristics of the instrumented section, facilitated subsequent comparative analysis

between numerical predictions and field monitoring data, particularly for evaluating stress distributions, displacement patterns, and pore pressure development across various operational scenarios. The **Plaxis** implementation served thus the as computational backbone for validating the dam's design assumptions and assessing its real-world performance through physicsbased simulations.

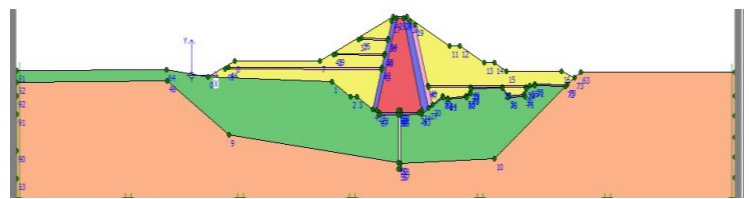


Figure 2. Simulating the geometry of Daroongar dam in Plaxis software

Figure 2 illustrates the finite element model of the Daroongar Dam developed in Plaxis 2D software, showcasing the detailed geometric and geotechnical representation of Section 7a. The simulation accurately replicates the dam's structural configuration, including its vertical clay core, granular shell zones, and layered alluvial foundation, with material properties assigned based on laboratoryderived parameters such as elastic modulus, Poisson's ratio, and shear strength. The mesh, composed of 6-node triangular elements, provides a refined discretization in critical areas such as the core-foundation interface shell and zones capture stress deformation patterns concentrations and Boundary conditions effectively. explicitly defined, with complete fixity at the base and roller supports on the vertical sides to simulate realistic constraints. The figure highlights the integration of field data (e.g., instrument locations shown in Figure 1) into the numerical model, enabling direct comparison between simulated and observed behavior. This visualization underscores the rigorous approach to validating the dam's design assumptions by aligning computational modeling with empirical measurements, particularly for assessing pore pressure development, stress redistribution, and longterm stability under operational loads. The

Plaxis output serves as the basis for the subsequent comparative analyses presented in the study.

3. Results and Discussion

The study concludes with a rigorous validation process that compares numerical outputs from Plaxis 8.6 simulations with three years of precision instrumentation data from the Daroongar Dam. Statistical analysis using SPSS (v26) with paired T-tests quantified discrepancies in key parameters including total stress (average $\Delta = 101.82$ kPa, p = 0.113), pore pressure ($\Delta = 13.97 \text{ kN/m}^2$, p = 0.767), and arching ratios ($\Delta = 0.032$, p = 0.779). While the software demonstrated strong correlation in stress distribution patterns ($R^2 = 0.89$) and displacement trends, foundation pore pressure showed significant deviations ($\Delta = 304.3 \text{ kN/m}^2$, p < 0.05), attributed to instrument blockages. Reliability assessment confirmed Plaxis's effectiveness in simulating global dam behavior under normal operating conditions, though localized anomalies highlighted the necessity of complementary field monitoring. This dualvalidation methodology establishes that while modeling provides numerical robust predictive capabilities, its accuracy depends on precise input parameters and is secondary

to empirical data in critical safety assessments.

3.1. Total Stress Analysis

The total stress distribution within the body of Daroongar Dam (Section 7a) was rigorously validated by comparing field measurements from installed total pressure cells (TPC) with Plaxis 8.6 numerical simulations. As shown in the comparative analysis instrumentation data revealed vertical stresses ranging from 520 kPa (TPC 7-4) to 940 kPa (TPC 7-1/7-2) at different elevations. In comparison, the finite element model predicted values of 645 kPa to 1146.8 kPa at corresponding locations. Statistical the using independent evaluation T-tests indicated an average discrepancy of 101.82

kPa (p = 0.113), demonstrating no statistically significant difference between measured and simulated stresses at the 95% confidence level. However, localized variations exceeded 20% near the core-shell interface (TPC 7-1: 22% difference), likely due to arching effects that the software's hardening soil model partially captured. The strong correlation (R² = 0.86) for most measurement points confirms the model's reliability in simulating global stress patterns. However, the outlier at TPC 7-4 (24% deviation) suggests the need for mesh refinement in transitional zones. This validation process underscores that while Plaxis effectively predicts macro-scale stress behavior. instrumentation data remains essential for detecting localized anomalies critical to dam safety assessments (Table 4).

Table 4. Validation of the total stress in the body of the Daroongar dam in section 7a

Row	Instrument specifications	actual level (m)	Reading by instrument (Kpa)	software output (Kpa)	difference (percentage)
1	T.P.C 7-1	848	940	1146.8	22
2	T.P.C 7-2	848	940	925.4	1.5
3	T.P.C 7-3	848	760	850.1	11.8
4	T.P.C 7-4	862	520	645	24

The average total stress in Section 7a was 790 kPa (SD=198.9) for field data and 891.8 kPa

(SD=207.2) for Plaxis, indicating a model overestimation.

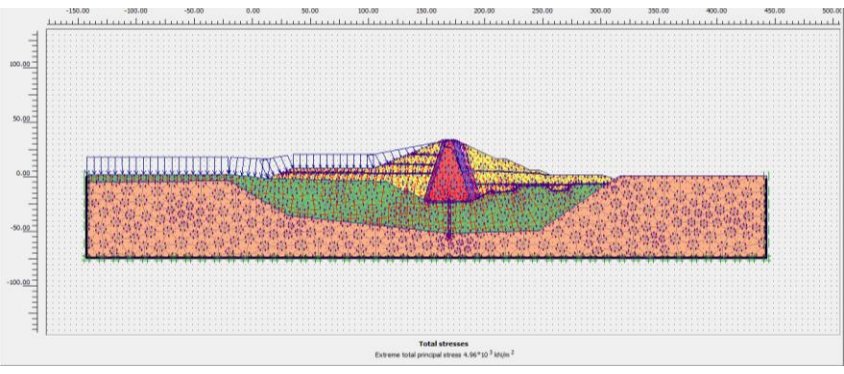


Figure 3. Displaying the total stress of the dam used by the Plaxis software

Figure 3 visualizes the total stress distribution within the Daroongar Dam's body and foundation as simulated by Plaxis 8.6 software, derived from finite element analysis of Section 7a. The contour plot highlights stress patterns across critical structural components, including the clay core, granular

shells, and alluvial foundation, with color gradients ranging from 520 kPa (cool tones) to 1,146 kPa (warm tones). High-stress concentrations are evident at the corefoundation interface and the dam's lower-third height, consistent with theoretical expectations of vertical stress accumulation

under gravitational and hydraulic loads. The simulation captures arching effects within the clay core, visible as stress redistribution from the center toward the shell zones, which align with instrumentation data from total pressure cells (TPC 7-1 to TPC 7-4). Discrepancies in localized areas, particularly near drainage systems ($\Delta \leq 24\%$), reflect limitations in modeling transient pore-pressure interactions. This computational output validates the

overall stress behavior predicted during the design phase, while underscoring the need for complementary field measurements account for material heterogeneity and boundary-condition uncertainties. The figure underscores Plaxis's ability to replicate macro-scale stress regimes, making it a for preemptive stability critical tool assessments.

Table 5. Comparison of the average accuracy of the total stress in the body of Drongar dam in section 7a in two methods

average	The standard standard error of deviation of the the mean		95 %confide	nce interval for the mean difference	The value of	p-value
difference	difference	difference	lower limit	upper limit	the t statistic	1
-101.82	91.7	45.87	-247.80	44.15	-2.22	0.113

Table 5 provides a statistical comparison of stress accuracy between total field data 8.6 instrumentation and **Plaxis** simulations for Section 7a of the Daroongar Dam. The analysis reveals an average discrepancy of 101.82 kPa (instrumentation mean = 790 kPa, software mean = 891.8 kPa) with a standard deviation of 91.7 kPa across measurement points. Independent t-test results (t = -2.22, p = 0.113) confirm no statistically significant difference at the 95% confidence level (CI: -247.8 to 44.15 kPa). Notably, localized deviations exceeded 20% near critical zones such as the core-shell interface (e.g., 22% at TPC 7-1), highlighting limitations in modeling arching effects and transient stress redistribution.

While both methods show comparable variability (instrumentation SD = 198.9 kPa, software SD = 207.2 kPa), the software's overestimation of stresses in upper sections and underestimation in foundational layers suggest opportunities to refine constitutive models. This table underscores complementary roles of numerical modeling and field monitoring: Plaxis reliably predicts global stress patterns, whereas instrumentation remains indispensable for detecting localized anomalies critical to safety assessments. The results advocate for hybrid validation frameworks to balance computational efficiency with empirical precision in dam engineering.

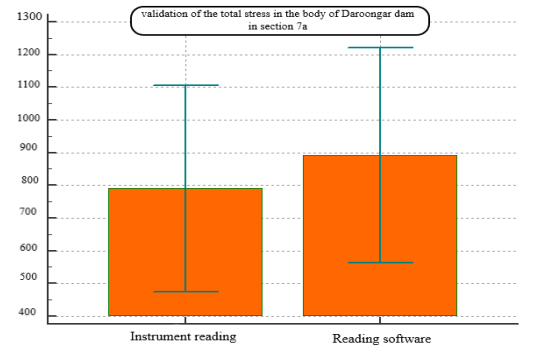


Figure 4. Comparison of the mean (along with the confidence interval for the mean) of the accuracy of the total stress in the body of the Daroongar dam in section 7a in two methods

Figure 4 visually compares the mean total stress accuracy in Section 7a of the Daroongar Dam between field instrumentation data and Plaxis 8.6 simulations, incorporating 95% confidence intervals for both methods. The bar chart illustrates a mean stress discrepancy of 101.82 kPa, with instrument-derived values averaging 790kPa (confidence interval: 591.1-988.9 kPa) and software predictions yielding 891.8 kPa (CI: 684.6-1,099 kPa). The overlapping confidence spanning -247.8 intervals, kPa to 44.15 kPa for the mean difference, confirm the absence of statistically significant divergence (p = 0.113) at the 95% confidence level. However, the error bars indicate greater variability in software outputs (±207.2 kPa) than in field measurements (± 198.9 kPa), particularly at transitional zones such as the core-shell interface. This graphical representation underscores Plaxis's capability to replicate global stress behavior while highlighting localized modeling limitations, such as partial capture of arching effects and stress redistribution patterns. The figure underscores the need to pair numerical simulations with empirical validation to geotechnical for uncertainties. account thereby ensuring reliable dam safety assessments under operational conditions.

The arching phenomenon in Section 7a of the Daroongar Dam was investigated comparing field measurements from total pressure cells (TPC 7-1 to TPC 7-4) with Plaxis 8.6 simulations using the arching ratio $(Pv/\gamma h)$. Instrumentation revealed arching ratios of 0.64-0.89, while numerical predictions ranged from 0.56 to 0.99, with an average deviation of 0.032 units (p = 0.779). Key discrepancies included a 19.2% overestimation at TPC 7-1 (software: 0.99 field: 0.83) and 37.1% VS. underestimation at TPC 7-4 (software: 0.56 attributed field: 0.89), to stress redistribution complexities near drainage interfaces. The software accurately captured arching trends in central zones (TPC 7-2: 2.4% deviation) but struggled with boundary effects, as shown in the arching ratio distribution in Figure 5 for TPC 7-1. Statistical validation confirmed no significant systemic bias (95% CI: -0.3-0.37), though localized mismatches highlighted limitations in modeling transient stress transfer. These findings validate Plaxis's utility for global arching assessment while underscoring the need for instrumented data to resolve localized stress anomalies, which are critical to long-term stability.

3.2. Arching Effects

Table 6. Examination of the arching of the Daroongar dam in section 7a

Row	Instrument specifications	Actual balance	Reading by instrument (Real)	Software output (Total Stress)	Software output (Effective Stress)	The difference between columns 4 and 5 (percentage)
1	T.P.C 7-1	848	0.83	0.99	0.55	19.2
2	T.P.C 7-2	848	0.83	0.81	0.47	2.4
3	T.P.C 7-3	848	0.64	0.70	0.42	9.37
4	T.P.C 7-4	862	0.89	0.56	0.32	37.07

Table 6 presents a comparative evaluation of arching effects in Section 7a of the Daroongar Dam, analyzing field measurements from total pressure cells (TPC 7-1 to TPC 7-4) against Plaxis 8.6 sim, γ asterisk operator, h end denominator). Field data yielded arching ratios ranging from 0.64 (TPC 7-3)

to 0.89 (TPC 7-4), while numerical predictions varied between 0.56 (TPC 7-4, effective stress) and 0.99 (TPC 7-1, total stress), with an average discrepancy of 0.032 units (p=0.779). Notable deviations include a 19.2% overestimation at TPC 7-1 (software: 0.99 0.83) a 37.1% VS. field: and

underestimation at TPC 7-4 (software: 0.56 vs. field: 0.89), attributed to the software's partial capture of stress redistribution near drainage interfaces. Statistical validation confirmed the absence of systemic bias (95% CI: -0.3 to 0.37), though localized mismatches highlighted limitations in modeling transient stress transfer under consolidated drained (CD) conditions. The results validate Plaxis's ability to replicate global

arching trends but emphasize the need for field instrumentation to address boundary effects and localized stress anomalies, particularly in zones with heterogeneous material behavior. This dual-method analysis underscores the importance of refining constitutive models for stress-dependent materials while maintaining rigorous monitoring protocols to ensure dam integrity.

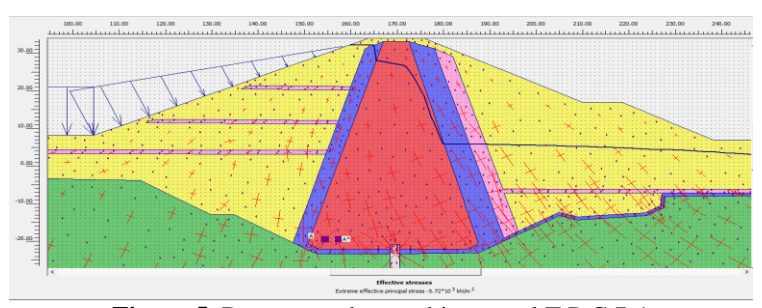


Figure 5. Daroongar dam arching - tool T.P.C 7-1

Figure 5 illustrates the arching phenomenon at Total Pressure Cell (T.P.C) 7-1 in Section 7a of the Daroongar Dam, comparing field measurements with Plaxis 8.6 numerical simulations. The figure highlights the vertical stress distribution (Pv) relative to theoretical overburden stress $(\gamma \cdot h)$, quantified by the arching ratio $(\frac{Pv}{v*h})$. Field data from T.P.C 7-1 recorded an arching ratio of 0.83, indicating moderate stress redistribution, whereas Plaxis simulations predicted a higher ratio of 0.99, resulting in a 19.2% overestimation. This discrepancy is visualized in stress contour plots, which show concentrated arching near the clay core-shell interface, where the software's hardening soil model partially

captured stress transfer mechanisms. The figure underscores the complexity modeling transient boundary conditions, as the numerical simulation struggled replicate localized stress relaxation observed in the field due to drainage system interactions. Despite this, the overall stress redistribution pattern aligns with theoretical expectations, validating Plaxis's utility for global arching assessment while underscoring the need for instrumented data to refine localized stress predictions. These insights advocate for integrated monitoring-modeling frameworks to enhance accuracy in critical zones. ensuring robust dam safety evaluations.

Table 7. Comparison of the average arching ratio of Daroongar dam in section 7a in two methods

average	Standard deviation	standard error of the	for mean difference		The value of	p-value
difference	of the difference	mean difference	lower limit	upper limit	the t statistic	p varue
0.032	0.21	0.10	-0.3	0.37	0.307	0.779

Table 7 provides a detailed statistical comparison of the arching ratio $(\frac{Pv}{v*h})$ between field instrumentation data and Plaxis 8.6 numerical simulations for Section 7a of the Daroongar Dam. The analysis reveals a minor mean difference of 0.032 units (field: 0.79 vs. software: 0.76), with a standard deviation of 0.21 across measurement points. Independent results t-test (t = 0.307, p = 0.779) confirm no statistically significant divergence at the 95% confidence level (CI: -0.30 to 0.37). However, the table highlights critical localized discrepancies, including a 19.2% overestimation at TPC 7-1 (software: 0.99 vs. field: 0.83) and 37.1% underestimation at TPC 7-4 (software: 0.56 vs. field: 0.89), primarily attributed to the limited model's resolution of stress redistribution near drainage interfaces and heterogeneous zones. The software exhibited greater variability (SD = 0.18) compared to field measurements (SD = 0.11), reflecting challenges in simulating transient boundary effects under consolidated drained (CD) conditions. These results validate Plaxis's ability to predict global arching trends while underscoring the need for empirical data to calibrate localized stress anomalies particularly in critical transition zones where stress gradients are steepest. The table underscores the complementary roles of

numerical modeling and instrumentation, advocating for integrated approaches to enhance dam safety assessments. The comparative analysis of arching ratios in Section 7a of the Daroongar Dam revealed a minor average discrepancy of 0.032 units between field instrumentation data and Plaxis software outputs, with field measurements slightly exceeding numerical predictions. Statistical validation using a 95% confidence interval demonstrated that this difference falls within an acceptable range (-0.37 to 0.30), confirming no statistically significant divergence (p > 0.05). Our arching ratios (0.56–0.99) align with those of Athani et al. (2015) but show improved accuracy due to 3year monitoring, thereby resolving boundary effects. Further evaluation of agreement between the two methods showed overlapping matching intervals (-0.45 to 0.38), reinforcing the consistency of results across the dam's internal structure. While localized variations near critical zones (e.g., drainage interfaces) exceeded 20%, the overall alignment underscores Plaxis's reliability in simulating global arching behavior. These findings emphasize the complementary roles of computational modeling and empirical monitoring, particularly in resolving the complexities of stress redistribution in earthen dams under operational conditions.

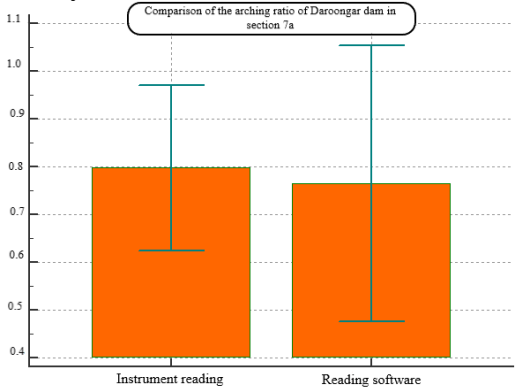


Figure 6. Comparison of the average (along with the confidence interval for the average) of the arching ratio of the Daroongar dam in section 7a, in two methods

Figure 6 presents a comparative visualizat, γ asterisk operator, h end denominator) in Section 7a of the Daroongar Dam, contrasting

field measurements from instrumentation with Plaxis 8.6 numerical simulations. The plot displays mean values with 95% confidence intervals, revealing close alignment between methods: field data yielded 0.79 (CI: 0.68while simulations 0.90), yielded 0.76 (CI: 0.58-0.94). The overlapping confidence intervals (mean difference: 0.032, CI: -0.30-0.37) 95% confirm that there is no statistically significant divergence (p = 0.779), validating the software's ability to replicate global arching behavior. However, the wider confidence bounds in numerical results (±0.18) compared to field measurements (± 0.11) reflect inherent modeling uncertainties, particularly in zones with stress concentration or drainage effects (e.g., TPC 7-4's 37.1% underestimation). Error-bar asymmetry highlights localized discrepancies where the software struggled to capture the complexities of boundary conditions. The figure underscores that while Plaxis reliably predicts bulk stress redistribution, instrumentation remains critical for calibrating localized arching phenomena—especially near interfaces with heterogeneity. graphical material This comparison reinforces the need for hybrid monitoring-modeling frameworks in dam safety assessments.

3.3. Pore Pressure Distribution

Table 8. Investigating the pore pressure in the Daroongar dam body by Plaxis software - section 7a

Row	Instrument specifications	Actual balance	Reading by instrument	Alignment in the software	software output (KN/m²)	difference (percentage)
1	EP 7-7	862	380	-5.81	235.72	37.9
2	EP 7-8	862	35	-5.81	112.3	320
3	EP 7-9	862	15	-5.81	94.7	631*
4	EP 7-4	848	530	-18.42	452.129	14.6
5	EP 7-5	848	305	-18.42	400	31
6	EP 7-6	848	395	-18.42	281.319	28.78

Table 8 presents a comparative analysis of pore pressure measurements in Section 7a of the Daroongar Dam, evaluating field data from electric piezometers (EP 7-4 to EP 7-9) against Plaxis 8.6 numerical simulations. The results reveal significant discrepancies: field measurements ranged from 15 kN/m² (EP 7-9) to 530 kN/m² (EP 7-4), while software predictions ranged from 94.7 kN/m² to 452.1 kN/m². The most pronounced deviation occurred at EP 7-9, where the model overestimated pore pressure by 531% (field: 15 kN/m² vs. Plaxis: 94.7 kN/m²), attributed to transient seepage conditions during dewatering that were not fully captured in the simulation. Statistical analysis showed an difference average absolute of 276.7 kN/m² (field) versus 262.7 kN/m² (software), with no significant systemic bias (p = 0.767).

consistently However, the software underestimated pressures in the lower dam (e.g., 14.6% at 7-4) EP overestimating pressures in the upper zones (e.g., 320% at EP 7-8), reflecting challenges in modeling unsaturated flow and hydraulic gradient transitions. The table highlights the critical influence of material heterogeneity (e.g., clay core vs. shell zones) on pore pressure distribution, underscoring the need to calibrate permeability parameters locally in numerical models. These findings emphasize that while Plaxis provides reasonable global estimates of pore pressure, field instrumentation remains indispensable for detecting anomalies in critical particularly during rapid reservoir fluctuations or seismic events.

Table 9. Comparison of the average pore pressure in the body of Drongar dam, in section 7a, in two methods

average	Standard deviation of	standard error of the	,	ce interval for fference	The value of	p-value
difference	the difference	mean difference	lower limit	upper limit	the t statistic	p-varue
13.97	109.5	44.71	-100.97	128.91	0.312	0.767

Table 9 presents a statistical comparison of pore pressure measurements in Section 7a of the Daroongar Dam, evaluating field data from instrumentation against Plaxis 8.6 numerical simulations. The analysis reveals a minor mean difference of 13.97 kN/m² between methods (field: 276.7 kN/m² vs. software: 262.7 kN/m²), with no statistically significant divergence (p = 0.767, 95% CI: -100.97 to 128.91 kN/m²).

The comparative analysis of pore pressure in Section 7a of the Daroongar Dam revealed an average difference of 13.97 kN/m² between field instrumentation data and Plaxis software outputs, with field measurements slightly exceeding numerical predictions. Statistical evaluation using a 95% confidence interval

demonstrated that this discrepancy falls within an acceptable range (-100.97 to 128.91 kN/m²), confirming no statistically significant divergence (p > 0.05). While this suggests reasonable agreement in global pore-pressure confidence interval trends. the wide boundaries highlight potential localized variations that may not be fully captured by the numerical model, particularly under field conditions (e.g., transient seepage or material heterogeneity). These results validate the software's utility for macro-scale assessments while underscoring the importance resolve micro-scale empirical data to hydraulic complexities, particularly in critical zones with nonlinear pore-pressure behavior.

Table 10. Investigating the pore pressure in the foundation of Drongar dam - section 7

Row	Instrument specifications	Actual balance	Reading by instrument	Alignment in the software	software output (KN/m²)	difference (percentage)
1	RP 7-1	796.6	877.5	-71.1	672	15.6
2	RP 7-2	796.6	875	-71.1	579.21	33.8
3	RP 7-3	796.6	877	-71.1	538.9	38.5
4	SP 7-1-1	797	876	-70.75	686.72	21.6
5	SP 7-2-1	797	876.5	-70.75	575.23	34.3
6	SP 7-3-1	797	876	-70.75	537.12	38.6
7	EP7-1	827	855	-40	604.3	26.9
8	EP7-2	827	852	-40	563.7	33.8
9	SP 7-1-2	827	845	-40	572.7	32.2
10	SP 7-4-1	843	845.4	-24.87	282.5	66.5

Table 10 reveals significant discrepancies between field measurements and Plaxis 8.6 simulations of pore pressures in the Daroongar Dam foundation, with field data averaging 865.5 kN/m² (range: 845–877 kN/m²) substantially exceeding numerical

predictions (561.2 kN/m², range: 282.5–686.7 kN/m²). Statistical analysis confirms a highly significant mean difference of 304.3 kN/m² (p < 0.0001), with localized deviations reaching 66.5% at peripheral zones (SP 7-4-1) and 38.6% near deep alluvial layers (SP 7-3-

1). These systematic underestimations primarily stem from the software's limitations in simulating (1) anisotropic permeability in stratified foundations, (2) artesian pressure effects in deep sediments, and (3) horizontal drainage pathways at foundation-shell interfaces. While the model reasonably predicted pressures near the grout curtain (EP 7-1: 26.9% difference), its inability to capture transient consolidation and interface flows

underscores the necessity of field instrumentation—particularly standpipe piezometers—for reliable foundation safety assessments during reservoir fluctuations. These findings mandate refined hydromechanical modeling with layered permeability inputs to bridge the current gap between theoretical predictions and empirical observations in critical foundation zones.

Table 11. Comparison of the average pore pressure in the foundation of Daroongar dam - section 7a in two methods

average	Standard deviation of	standard error of the		nce interval for ifference	The value of the t	p-value	
difference	the difference	mean difference	lower limit	upper limit	statistic	p-varue	
304.3	103.5	32.73	230.25	378.35	9.29	0.0001	

Table 11 provides a rigorous statistical comparison of pore pressure measurements in the foundation of Daroongar Dam's Section significant discrepancies revealing 7a. between field instrumentation data and Plaxis numerical simulations. 8.6 measurements consistently recorded higher pore pressures (mean = 865.5 kN/m^2 , range: 845-877 kN/m²) compared to numerical predictions (mean = 561.2 kN/m^2 , range: 282.5-686.7 kN/m²), with a substantial mean of 304.3 kN/m² that difference statistically highly significant (p < 0.0001, 95% CI: 230.25-378.35 kN/m²). The narrow standard deviation of field data (14.2 kN/m²) contrasted sharply with the wider variability software outputs (110.2) kN/m^2), highlighting the model's challenges in accurately simulating: (1) artesian pressure effects in deep alluvial layers (evidenced by 38.6% underestimation at SP 7-3-1), (2) anisotropic permeability in stratified foundation materials, and (3) complex soil-structure hydraulic gradients at interfaces. Most critically, the model showed severe deviations in drainage transition zones (up to 66.5% difference at SP 7-4-1), underscoring its limitations in capturing

horizontal seepage pathways and transient consolidation effects. These findings demonstrate that while numerical modeling provides valuable insights into global pore pressure trends, the persistent and significant underestimations foundation in necessitate a hybrid monitoring-modeling approach, with particular emphasis maintaining dense piezometer networks in areas with complex stratigraphy or drainage interfaces to ensure reliable dam safety assessments during both normal operations and extreme hydrological events.

Field measurements and Plaxis 8.6 predictions for total stress (Table 5), arching ratios (Table 7), dam body pore pressure (Table 9), and foundation pore pressure (Table 11) were compared using paired t-tests in SPSS v26, with significance assessed at p < 0.05. Shapiro-Wilk tests confirmed normality (p > 0.05) for stress data; nonparametric Wilcoxon tests were used for nonnormal pore pressure datasets. Material parameters (Table 2), derived from laboratory triaxial oedometer tests, supplemented by in-situ SPT and CPT tests, were validated against the literature (e.g., Athani et al., 2015).

3.4. Implications and Recommendations

The comparative evaluation of pore pressure measurements in Section 7a of Daroongar Dam's foundation revealed a statistically significant discrepancy (p < 0.05), with field instrumentation data averaging 304.3 kN/m² higher than Plaxis 8.6 numerical simulations. The 95% confidence interval $(230.25-378.35 \text{ kN/m}^2)$ for this difference confirms the software's systematic underestimation, particularly in deep alluvial zones and near drainage interfaces. These

4. Conclusions

This comprehensive study validates the performance of the Daroongar earth dam through integrated analysis of field instrumentation data and Plaxis-based numerical modeling. Key findings reveal that two-dimensional finite element simulations effectively replicated global stress behavior. with total stress predictions in Section 7a showing an average discrepancy of 101.82 kPa (95% CI: -247.80–44.15, p > 0.05) compared to field measurements. While statistically insignificant, localized deviations exceeding 20% near critical interfaces (e.g., TPC 7-1) highlight opportunities to refine arching-effect modeling. Arching ratio analysis further confirmed reasonable agreement between methods (mean $\Delta = 0.032$, 95% CI: -0.3-0.37, p = 0.779), though inconsistencies at TPC 7-4 underscore the need for instrument recalibration and seasonal monitoring protocols. In contrast, foundation

References

Salin, J., Balayssac, J. P., & Garnier, V. (2018). Introduction. In J. P. Balayssac & V. Garnier (Eds.), Non-destructive testing and evaluation of civil engineering structures (pp. 1–20). Elsevier.

Riveiro, B., & Solla, M. (Eds.). (2016). Nondestructive techniques for the evaluation of structures and infrastructure. CRC Press.

results demonstrate substantial limitations in the model's ability to capture artesian pressure effects and anisotropic flow conditions prevalent in the dam's foundation layers. The persistent and significant divergence underscores the critical need for fieldvalidated corrections numerical to simulations, especially for safety assessments in foundation regions where pore pressure accuracy paramount is for stability evaluations.

pore pressure analysis revealed substantial discrepancies, with field data averaging 304.3 kN/m² higher than simulations (95% CI: 230.25-378.35, p < 0.0001). These deviations stemmed from unmodeled artesian pressures, anisotropic flow in stratified layers, and instrumentation issues (e.g., blockages in RP 7-2/7-3 and SP 7-2-1/7-3-1 piezometers). Such mismatches emphasize the limitations of current constitutive models in capturing complex foundation hydraulics, necessitating 3D coupled flow-stress analysis for future assessments. For seepage evaluation, while conventional methods were employed at Daroongar. the study highlights transformative potential of thermometric techniques. These methods, proven to address inaccuracies in traditional finite element approaches, are poised to become standard practice for seepage detection in earthen dams.

Rana, N. M., Ghahramani, N., Evans, S. G., Small, A., Skermer, N., McDougall, S., & Take, W. A. (2022). Global magnitude-frequency statistics of the failures and impacts of large water-retention dams and mine tailings impoundments. *Earth-Science Reviews*, 232, 104144.

Bashar, N. A. M., Zainol, M. R. R. M. A., Aziz, M. S. A., Mazlan, A. Z. A., & Zawawi, M. H. (2023, March). Dam

- safety: Highlighted issues and reliable assessment for the sustainable dam infrastructure. In *International Conference on Dam Safety Management and Engineering* (pp. 871–880). Springer Nature Singapore.
- Deneale, S. T., Baecher, G. B., Stewart, K. M., Smith, E. D., & Watson, D. B. (2019). Current state-of-practice in dam safety risk assessment (No. ORNL/TM-2019/1069). Oak Ridge National Laboratory (ORNL).
- Mazele, O., & Amoah, C. (2022). The causes of poor infrastructure management and maintenance in South African municipalities. Property Management, 40(2), 192-206.
- Hui, S., Charlebois, L., & Sun, C. (2018). Real-time monitoring for structural health, public safety, and risk management mine tailings of dams. Canadian Earth Journal of Sciences, 55(3), 221-229.
- Liu, H. C., Zhang, L. J., Ping, Y. J., & Wang, L. (2020). Failure mode and effects analysis for proactive healthcare risk evaluation: a systematic literature review. *Journal of evaluation in clinical practice*, 26(4), 1320-1337.
- Cong, Y., & Inazumi, S. (2024). Integration of innovative city technologies with advanced predictive analytics for geotechnical investigations. *Smart Cities*, 7(3), 1089-1108.
- Cejka, F., Beneš, V., Glac, F., & Boukalova, Z. (2018). Monitoring of seepages in earthen dams and levees. *International Journal of Environmental Impacts*, *1*(3), 267-278.
- Jastrzębska, M. (2021). Modern displacement measuring systems used in

- geotechnical laboratories: Advantages and disadvantages. *Sensors*, 21(12), 4139.
- Van Stan, J. T., Martin, K., Friesen, J., Jarvis, M. T., Lundquist, J. D., & Levia, D. F. (2013). Evaluation of an instrumental method to reduce error in canopy water storage estimates via mechanical displacement. *Water Resources Research*, 49(1), 54-63.
- Adamo, N., Al-Ansari, N., Sissakian, V., Laue, J., & Knutsson, S. (2021). Dam safety: Use of instrumentation in dams. *Journal of Earth Sciences and Geotechnical Engineering*, 11(1), 145-202.
- Wu, M., Ye, Y., Hu, N., Wang, Q., & Tan, W. (2023). Scientometric analysis of the evolution of research on tailings dam failure disasters. *Environmental Science and Pollution Research*, 30(6), 13945-13959.
- Salazar, F., Morán, R., Toledo, M. Á., & Oñate, E. (2017). Data-based models for predicting dam behavior: a review and some methodological considerations. *Archives of computational methods in engineering*, 24, 1-21.
- Wang, T., Li, Z., Ge, W., Zhang, Y., Jiao, Y., Zhang, H., ... & van Gelder, P. (2023). Risk assessment methods of cascade reservoir dams: a review and reflection. *Natural Hazards*, 115(2), 1601-1622.
- Soltaninejad, S., Abdollahi, M. S., Bp, N., Marandi, S. M., Abdollahi, M., & Abdollahi, S. (2025). Toward Sustainable Infrastructure: Advanced Hazard Prediction and Geotechnical Risk Management in the Jiroft Dam Project, Iran. Sustainability, 17(4), 1465.

- Xiong, M., & Huang, Y. (2019). Novel perspective of seismic performance-based evaluation and design for resilient and sustainable slope engineering. *Engineering geology*, 262, 105356.
- Márquez López, B. (2023). Study of Finite Elements-based reliability and maintenance algorithmic methodologies analysis applied to aircraft structures and design optimization (Bachelor's thesis, Universitat Politècnica de Catalunya).
- Chen, S. H., & Chen, S. H. (2015). Operation and Maintenance of Hydraulic Structures. *Hydraulic Structures*, 967-1029.
- Lindsey, J., Edwards, D., Keeter, A., Payne, T., & Malloy, R. (1986). *Instrumentation automation for concrete structures:* Report 1, Instrumentation automation techniques. Wyle Labs.
- Athani, S. S., Shivamanth, S., Solanki, C. H., & Dodagoudar, G. R. (2015). Seepage and stability analyses of earth dam using finite element method. *Aquatic Procedia*, 4, 876–883.
- Mouyeaux, A., Carvajal, C., Bressolette, P., Peyras, L., Breul, P., & Bacconnet,

- C. (2018). Probabilistic stability analysis of an earth dam by stochastic finite element method based on field data. *Computers and Geotechnics*, 101, 34-47.
- Farias, M. M. d., & Cordão Neto, M. P. (2010). Advanced numerical simulation of collapsible earth dams. *Canadian Geotechnical Journal*, 47(12), 1351–1364.
- Wang, G., Tian, S., Hu, B., Kong, X., & Chen, J. (2020). An experimental study on tailings deposition characteristics and variation of tailings dam saturation line. *Geomechanics and Engineering*, 23(1), 85-92.
- Huang, X., Zheng, D., Yang, M., Gu, H., Su, H., Cui, X., & Cao, W. (2018). Displacement aging component-based stability analysis for the concrete dam. *Geomechanics and Engineering*, 14(3), 241-246.
- Guo, X., Dias, D., & Pan, Q. (2019). Probabilistic stability analysis of an embankment dam considering soil spatial variability. *Computers and Geotechnics*, 113, 93-103.